

Synthesis, structural characterization and application of a 2D coordination polymer of Mn-terephthalate as a heterogeneous catalyst for olefin oxidation



Mojtaba Bagherzadeh^{a,*}, Fatemeh Ashouri^a, Marijana Đaković^b

^a Department of Chemistry, Sharif University of Technology, P.O. Box 11155-3516, Tehran, Iran

^b Department of Chemistry, Faculty of Science, University of Zagreb, HR-10000 Zagreb, Croatia

ARTICLE INFO

Article history:

Received 31 August 2013

Accepted 22 November 2013

Available online 9 December 2013

Keywords:

Two-dimensional polymer

Coordination polymer of manganese

Olefin oxidation

Heterogeneous catalyst

ABSTRACT

A metal–organic coordination polymer of $[\text{Mn}_3(1,4\text{-benzenedicarboxylate})_3(\text{DMF})_4]$ ($[\text{Mn}_3(\text{BDC})_3(\text{DMF})_4]_n$) was synthesized and characterized by IR spectra, elemental analysis (CHN), thermal gravimetric analysis (TGA) and single crystal X-ray diffraction analysis. The structure of $[\text{Mn}_3(\text{BDC})_3(\text{DMF})_4]_n$ is a 2D-periodic framework based on Mn(II)-terephthalate secondary building units (SBUs). The catalytic oxidation of various olefins was effectively carried out with $[\text{Mn}_3(\text{BDC})_3(\text{DMF})_4]_n$. Moreover, the influence of key reaction parameters, including the solvents, reaction temperatures and nature of oxidant were studied. The optimized conditions were achieved by TBHP as the efficient oxidant in 1,2-dichloroethane solvent at 75 °C. Finally, this catalyst was used for four cycles efficiently without a significant loss of yield.

© 2013 Elsevier Ltd. All rights reserved.

1. Introduction

Metal–organic coordination polymers (CPs) are prominent materials in the fields of supramolecular chemistry and crystal engineering, through their specific structural topologies, properties and reactivities [1–5]. Since 1916, when Shibata first used the term ‘Coordination Polymer’ to describe dimers and trimers of various cobalt(II) ammine nitrates [6], several research groups have reported a wide variety of CPs, such as 1D-chains and ladders, 2D grids and 3D microporous networks [7–11]. Extensive studies on the design, synthesis and structural analysis of metal–organic CPs are performed due to their potential applications in materials, electrochemistry, catalysis, gas adsorption, magnetism, non-linear optics, luminescence, photoluminescent and photo-electrics and as well as many other fields [12–18].

Depending on the nature of the system used, either infinite extended polymeric or discrete closed oligomeric structures can be generated. Despite the upsurge in the construction of various supramolecular structures, the control of dimensionality is still a challenging task in this field and often it is difficult to predict the final product [19,20]. The active nature of metal–ligand bonds, various coordination geometries of the metal centers, nature and coordinating topologies of the ligands used, metal–ligand ratio, nature of the counter ions and various experimental conditions,

such as solvent, temperature and crystallization methods, influence the supramolecular architectures [21–27]. The framework structure of CPs primarily depends upon the coordination preferences of the central metal ions and the functionality of the ligands. Therefore, self-assembly of the metal ion with organic spacers as bridging units is an efficient approach to prepare CPs. It is widespread that the careful selection of the bridging ligands is one of the major factors for the synthesis of the CPs with novel structures. As a type of multidentate ligands, carboxylate derived ligands play an essential role in coordination chemistry and have attracted great attention because they can adopt various binding modes (i.e. monodentate, chelating, bridging) and have been widely manipulated to create polynuclear metal complexes with intriguing structural motifs [28–31].

CPs based on carboxylate ligands are especially suitable for catalysis, leading to a new generation of solid catalysts with uniform catalytic sites and open channel structures for different catalytic reactions [32,33]. Oxidation catalysis represents an influential research area because it represents the core of a variety of chemical processes for producing bulk and fine chemicals. Thus, the design of active, selective and recyclable heterogeneous catalysts is a challenging objective in the field of oxidation catalysis. Here, we report the synthesis, structural characterization and thermal stability of the manganese terephthalate CPs, $[\text{Mn}_3(\text{BDC})_3(\text{DMF})_4]_n$. The catalytic efficacy of this complex towards the epoxidation of a variety of alkenes in different solvents using *tert*-butyl hydroperoxide (TBHP) as an oxidant was evaluated.

* Corresponding author. Tel.: +98 21 66165354; fax: +98 21 66012983.

E-mail address: bagherzadeh@sharif.edu (M. Bagherzadeh).

2. Experimental

2.1. Materials and instruments

Since all the reagents and solvents for the synthesis and analysis were commercially available, they were used as received without further purification. The CHN elemental analysis of the compound was obtained from a Carlo ERBA Model EA 1108 analyzer. The FT-IR spectrum was obtained by utilizing a Unicam Matson 1000 FT-IR spectrophotometer using KBr disks at room temperature. Thermogravimetric analysis was performed on a Perkin Elmer TGA7 analyzer in an N₂ atmosphere with a heating rate of 5 °C min⁻¹. XRD patterns were recorded on a Rigaku D-max C III, X-ray diffractometer using Ni-filtered Cu K α radiation. Inductively coupled plasma (ICP) was performed by an ICP-MS HP 4500. The products of the olefin oxidation reactions were determined and analyzed by an HP Agilent 6890 gas chromatograph equipped with an HP-5 capillary column (phenylmethylsiloxane 30 m \times 320 μ m \times 0.25 μ m) and a flame-ionization detector.

2.2. Synthesis of [Mn₃(BDC)₃(DMF)₄]_n

A solution of 1,4-benzenedicarboxylic acid (H₂BDC) (166 mg, 1 mmol) in 5 mL DMF was added to a DMF solution (5 mL) of MnCl₂·6H₂O (239 mg, 1 mmol) in a small sample tube. The solution was heated for 48 h at 80 °C without any stirring or shaking, and then the temperature was gradually decreased to 60 °C (2 °C/hour). After 2 days, white crystals of [Mn₃(BDC)₃(DMF)₄]_n (89% yield based on H₂BDC) were collected and removed from the vial. The crystals were washed with DMF (3 mL, 2 times) and dried in air to yield the pure product. *Anal. Calc.* for C₃₆H₄₀Mn₃N₄O₁₆: C, 45.54; H, 4.25; N, 5.90. *Found*: C, 45.67; H, 4.01; N, 5.87%. FT-IR (KBr 4000–400 cm⁻¹): 3471 (br), 3422 (br), 2936 (w), 2372 (w), 1643 (s), 1615 (s), 1555 (m), 1381 (s), 1104 (m), 886 (w), 818 (m), 750 (s), 625 (m), 516 (m).

2.3. Single crystal X-ray crystallography

Selected crystal data of [Mn₃(BDC)₃(DMF)₄]_n is given in Table 1. A single crystal of the complex was mounted in a random orientation on a glass fiber. Data collection was carried out at 296 K on an Oxford Diffraction X Calibur four-circle kappa geometry single-crystal diffractometer with a Sapphire 3 CCD detector, using a graphite monochromated Mo K α (λ = 0.71073 Å) radiation, and applying the CrysAlis Software system. The crystal-detector distance was 50 mm. Data reduction, including absorption correction, was done by the CrysAlice RED program [34]. The structure was solved by direct methods implemented in the SHELXS-97 program. The coordinates and the anisotropic displacement parameters for all non-hydrogen atoms were refined by full-matrix least-squares methods based on F^2 values using the SHELXL-97 program. All hydrogen atoms were placed in geometrically idealized positions and constrained to ride on their parent C atoms with C–H = 0.93 and 0.96 Å for CH and CH₃, respectively, and with U_{iso} (H) = $k \times U_{\text{eq}}$ (C), where k = 1.2 for CH H atoms and k = 1.5 for CH₃ H atoms [35]. Graphical work was performed via OLEX2 [36]. The thermal ellipsoids were drawn at the 50% probability level.

2.4. Catalytic methods

2.4.1. General procedure for olefin oxidation

For the heterogeneous oxidation of olefins, the reactions were carried out in a magnetically stirred two necked round-bottom flask fitted with a condenser, and placed in a temperature controlled oil bath. Typically, 1 mmol of the substrate was taken in

Table 1

Crystal data and details of the structure determination for [Mn₃(BDC)₃(DMF)₄]_n.

Coordination polymer	[Mn ₃ (BDC) ₃ (DMF) ₄] _n
Empirical formula	C ₃₆ H ₄₀ Mn ₃ N ₄ O ₁₆
Formula weight	945.98
Color and habit	colorless, prism
Crystal system	triclinic
space group	$P\bar{1}$
Crystal dimensions (mm)	0.16 \times 0.20 \times 0.56
<i>Unit cell parameters</i>	
<i>a</i> (Å)	9.9420(3)
<i>b</i> (Å)	12.7869(4)
<i>c</i> (Å)	16.6357(5)
α (°)	74.479(2)
β (°)	88.985(2)
γ (°)	87.228(32)
<i>V</i> (Å ³)	2035.3(1)
<i>Z</i>	2
<i>D</i> _{calc} (g cm ⁻³)	1.549
μ (mm ⁻¹)	0.992
θ (°)	4.21–30.00
<i>h</i> , <i>k</i> , <i>l</i> range	–13, 13; –17, 17; –23, 23
Scan type	ω
<i>F</i> (000)	974
No. reflections collected	21491
No. independent reflections	11829
No. observed reflections, $I > 2\sigma(I)$	8450
No. refined parameters	551
<i>R</i> ^a , <i>wR</i> ^b [$I \geq 2\sigma(I)$]	0.0650, 0.0416
<i>R</i> , <i>wR</i> (all data)	0.1175, 0.1118
<i>g</i> ₁ , <i>g</i> ₂ in <i>w</i> ^c	0.0664, 0.000
Goodness of fit on F^2 , <i>S</i> ^d	1.023
Max., min. electron density (e Å ⁻³)	0.566, –0.309
Maximum Δ/σ	0.001
Range of transmission factors min, max	0.633, 0.865
Extinction coefficient	none

$$^a R = \sum ||F_o| - |F_c|| / \sum |F_o|.$$

$$^b wR = [\sum (F_o^2 - F_c^2)^2 / \sum w(F_o^2)^2]^{1/2}.$$

$$^c w = 1/[\sigma^2(F_o^2) + \{(g_1 P)^2 + g_2 P\}] \text{ where } P = (F_o^2 + 2F_c^2)/3.$$

$$^d S = \sum [w(F_o^2 - F_c^2)^2 / (N_{\text{obs}} - N_{\text{param}})]^{1/2}.$$

2 mL solvent, followed by the addition of 3 mg catalyst (0.01 mmol Mn) and then, the mixture was heated to 75 °C. The reaction was begun with the addition of *tert*-butyl hydroperoxide (equimolar with respect to substrate). The products from the reaction mixture were analyzed by gas chromatography in the presence of chlorobenzene as an internal standard and were identified on comparison with known standards.

2.4.2. General procedure for the recyclability of the [Mn₃(BDC)₃(DMF)₄]_n catalyst in the oxidation reaction

The recyclability of the [Mn₃(BDC)₃(DMF)₄]_n catalyst was investigated in the oxidation reaction of styrene in the presence Mn/TBHP in 1,2-dichloroethane at 75 °C for 9 h. After the first catalytic reaction, the solid catalyst was easily isolated by centrifuge and recovered on being washed with solvent and dried at room temperature. Afterwards, the catalyst was used for the next run under the same reaction conditions.

3. Result and discussion

3.1. X-ray analysis of [Mn₃(BDC)₃(DMF)₄]_n

Single-crystal X-ray structure analysis revealed that [Mn₃(BDC)₃(DMF)₄]_n crystallizes in the triclinic $P\bar{1}$ space group (Table 1). Distinct from the aforementioned reported MOF structures based on Mn(II)-terephthalate SBUs composed of infinite Mn–O SBUs, the structure of [Mn₃(1,4-BDC)₃(DMF)₄]_n is a 2D-periodic framework composed of discrete SBUs, each of which is constructed from Mn^{II}O₆ corner shared octahedra (Fig. 1).

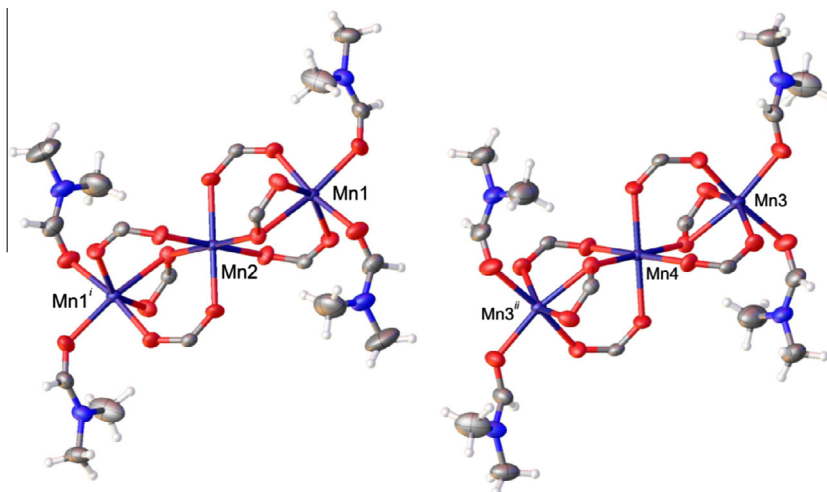


Fig. 1. ORTEP diagram of two symmetrically independent SBUs of $[\text{Mn}_3(\text{BDC})_3(\text{DMF})_4]_n$; the benzene rings of 1,4-BDC are omitted for clarity. (i) $-x - 1, 1 - y, -z - 1$; (ii) $-x, -y, -z$.

There are two discrete symmetrically independent SBUs in the crystal structure, which are further mutually linked by benzene units from 1,4-benzendicarboxylate links, furnishing a 2D framework in the (011) plane. Both types of symmetrically independent SBUs comprise three manganese(II) ions, two sitting in general positions (Mn1 and Mn3) and one at a center of inversion (Mn2 or Mn4), see Fig. 1.

The Mn(II) ions located in general positions, Mn1 and Mn3, are surrounded by two DMF oxygens in equatorial sites (O1A and O1B, and O1C and O1D, respectively) and four oxygens originating from 1,4-benzendicarboxylate, completing the octahedral coordination sphere, while the Mn(II) ions at inversion centers, Mn2 and Mn4, are coordinated by all six oxygen atoms originating only from carboxylate groups. Two carboxylate groups bridging the Mn(II) ions within the SBUs are coordinated to the metal centers, two in mode B and four in mode A (Fig. 2), contributing to the distortions of the Mn octahedra.

The main differences between the two SBUs, apart from the bond distances and angles of the corresponding coordination spheres, *i.e.* Mn1 and Mn3, and Mn2 and Mn4, are observed in the spatial orientations of the coordinated carboxylate groups and DMF molecules as well as in the mutual orientations of the Mn polyhedral within the SBUs. Selected bond distances and bond angles are listed in Table 2. All the Mn–O bond distances, varying from 2.113(2) to 2.302(2) Å, are comparable with the corresponding ones observed in MOF-73 [37] and the Mn(II) MOFs reported by Zheng and co-workers [38].

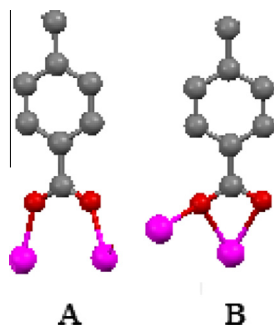


Fig. 2. Different coordination modes of 1,4-benzendicarboxylate observed in $[\text{Mn}_3(\text{BDC})_3(\text{DMF})_4]_n$.

Yang et al. revealed that in the assembly of coordination polymers, the different synthetic conditions, such as temperature, solvent and solvent mixture ratio, did not significantly influence the assembly [39]. However, in comparison with the Mn-terephthalate coordination polymer reported in this study and the one proposed by Yang et al. it was observed that slightly different in synthesis conditions lead to slightly different SBUs. In the synthesized $[\text{Mn}_3(\text{BDC})_3(\text{DMF})_4]_n$, two DMF molecules of solvent coordinate to the Mn1 center and block the crystal growth in this plane. Consequently, one two-dimensional coordination polymer was obtained, while coordination polymers composed of 1,4-benzendicarboxylic acid and Mn metal are three-dimensional polymers in all previous reports [37–39].

Two different modes of mutual linkage of the SBUs into the 2D framework are observed, and in both of these the SBUs are connected by only one carboxylate bridge between them (Fig. 2). Along the crystallographic [011] direction, the carboxylate bridges link two closest polyhedral of two neighboring SBUs, while in the [100] and [111] directions the furthest two polyhedral of two adjacent SBUs are mutually interconnected (Fig. 3).

In comparison with MOF-73 [37] and the one previously reported by Zheng and co-workers [38], we found that the Mn compound presented in this paper crystallizes in a different space group and possesses a distinct framework structure. However, the resultant channels are of comparable dimensions with those reported previously, *viz.* 0.98×1.80 nm for $[\text{Mn}_3(\text{BDC})_3(\text{DMF})_4]_n$ versus 1.06×1.73 nm for the MOF-73 [37] and 0.95×1.79 nm for the Zheng sample [38], suggesting quite a rigid host framework of $[\text{Mn}_3(\text{BDC})_3(\text{DMF})_4]_n$ (Fig. 4).

3.2. Thermal investigation

The thermal stability of $[\text{Mn}_3(\text{BDC})_3(\text{DMF})_4]_n$ was investigated by thermogravimetric analysis (TGA) at a heating rate of 5 °C/min in N_2 in the temperature range 30–600 °C (Fig. 5). The complex was thermally stable up to approx. 150 °C, indicating the absence of solvent molecules in the crystal structure. The first major mass loss step of 12.86%, that occurred in the temperature range 150–190 °C, was attributed to the removal of 1.5 DMF molecules per formula unit (calcd. 11.80%), and upon further heating there was no mass loss until the structure collapsed at approx. 560 °C. It is obvious that the thermal stability of the CP reported in this paper is greater than that of other CPs reported previously [17,18].

Table 2
Selected bond lengths (Å) and angles (°) for $[\text{Mn}_3(\text{BDC})_3(\text{DMF})_4]_n$.

Bond length(Å)		Bond angles (°)			
Mn1–O1A	2.228(2)	O1A–Mn1–O1B	88.63(7)	O1C–Mn3–O1D	89.22(8)
Mn1–O1B	2.165(2)	O1A–Mn1–O2 ⁱ	169.62(7)	O1C–Mn3–O4	82.17(8)
Mn1–O2	2.113(2)	O1A–Mn1–O6	82.55(7)	O1C–Mn3–O7	173.72(7)
Mn1–O6	2.125(2)	O1A–Mn1–O9	90.07(7)	O1C–Mn3–O11	88.23(7)
Mn1–O9	2.288(2)	O1A–Mn1–O10	83.77(7)	O1C–Mn3–O12	85.47(8)
Mn1–O10	2.302(2)	O1B–Mn1–O2 ⁱ	82.85(7)	O1D–Mn3–O4	109.39(8)
		O1B–Mn1–O6	101.41(8)	O1D–Mn3–O7	84.98(7)
Mn2–O1	2.125(2)	O1B–Mn1–O9	165.14(8)	O1D–Mn3–O11	153.55(7)
Mn2–O5	2.147(2)	O1B–Mn1–O10	107.90(7)	O1D–Mn3–O12	96.60(7)
Mn2–O9	2.223(2)	O2 ⁱ –Mn1–O6	104.91(7)	O4–Mn3–O7	97.45(8)
		O2 ⁱ –Mn1–O9	96.64(6)	O4–Mn3–O11	96.32(6)
Mn3–O1C	2.281(2)	O2 ⁱ –Mn1–O10	93.17(7)	O4–Mn3–O12	150.92(7)
Mn3–O1D	2.135(2)	O6–Mn1–O9	93.10(6)	O7–Mn3–O11	98.04(6)
Mn3–O4	2.115(2)	O6–Mn1–O10	147.22(7)	O7–Mn3–O12	97.59(7)
Mn3–O7	2.127(2)	O9–Mn1–O10	57.25(6)	O11–Mn3–O12	89.22(8)
Mn3–O11	2.288(2)	O1–Mn2–O1 ⁱ	180.00	O3–Mn4–O3 ⁱⁱ	180.00
Mn3–O12	2.299(2)	O1–Mn2–O5	86.26(7)	O3–Mn4–O8	92.72(7)
		O1–Mn2–O5 ⁱ	93.74(7)	O3–Mn4–O8 ⁱⁱ	87.28(7)
Mn4–O3	2.118(2)	O1–Mn2–O9	88.99(7)	O3–Mn4–O11	88.44(6)
Mn4–O8	2.156(2)	O1–Mn2–O9 ⁱ	91.01(7)	O3–Mn4–O11 ⁱⁱ	91.56(6)
Mn4–O11	2.221(2)	O5–Mn2–O5	180.00	O8–Mn4–O8 ⁱⁱ	180.00
		O5–Mn2–O9	88.29(6)	O8–Mn4–O11	91.02(7)
		O5–Mn2–O9 ⁱ	91.71(6)	O8–Mn4–O11 ⁱⁱ	88.98(7)
		O9–Mn2–O9 ⁱ	180.00	O11–Mn4–O11 ⁱ	180.00

(i) $-x-1, 1-y, -z-1$; (ii) $-x, -y, -z$.

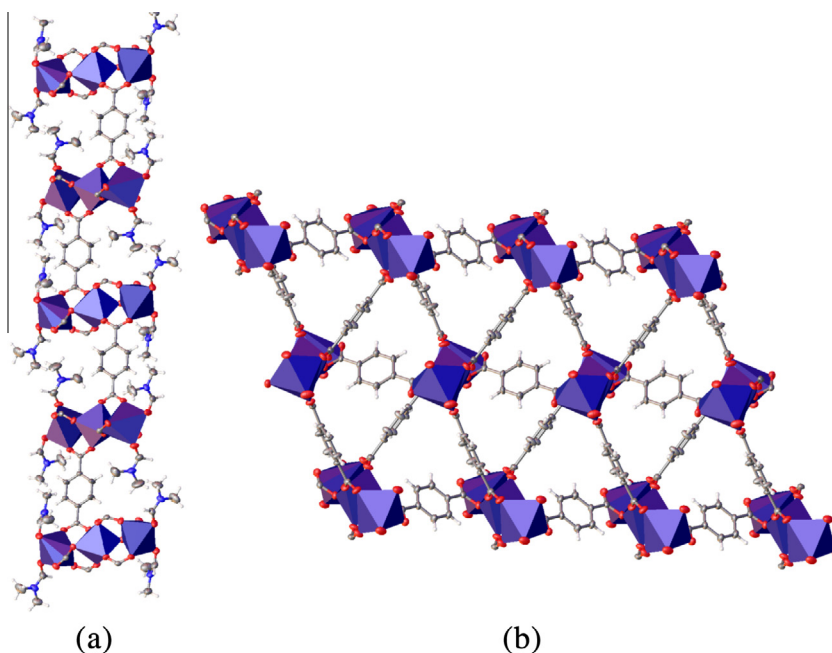


Fig. 3. Representation of the SBUs along the [011] direction (a); a view of the crystalline framework in the (011) plane with Mn shown as polyhedral and SBUs linked together via benzene rings of 1,4-benzenedicarboxylate (b).

3.3. Catalytic oxidation of olefins

Oxidation of C=C double bonds constitutes a significant reaction in organic chemistry that can lead to a diverse range of derivatives. Therefore, the catalytic activity of $[\text{Mn}_3(\text{BDC})_3(\text{DMF})_4]_n$ was examined for olefins oxidation. In order to find suitable reaction conditions to achieve the maximum oxidation of olefins, the effect of oxidant, solvent and temperature of the reaction were studied. Before carrying out a detailed study on the catalytic oxidation of various olefins, as a preliminary study we first optimized the reaction conditions by choosing styrene as a model substrate.

It is obvious that the solvent plays a crucial and decisive role in the catalytic behavior of a catalyst. Therefore, the impact of the

solvent nature in the catalytic oxidation of styrene was examined in the current catalytic system (Table 3). It was found the styrene oxidation reaction displayed the highest reactivity and selectivity when the reaction was performed in 1,2-dichloroethane media; methanol and DMF were not the most suitable solvents for the Mn-terephthalate coordination polymer. The efficiency of the catalysts in different solvents decreases in the order: 1,2-dichloroethane > acetonitrile > DMF > methanol > acetonitrile/methanol mixture. The result indicates the significant role of a suitable solvent for the titled oxidation reactions (conversion 2–96%).

The Mn complex alone is not capable of epoxidating olefins, even with substantial amounts of $[\text{Mn}_3(\text{BDC})_3(\text{DMF})_4]_n$. Therefore, in order to study the effect of oxidants on the catalytic activity of

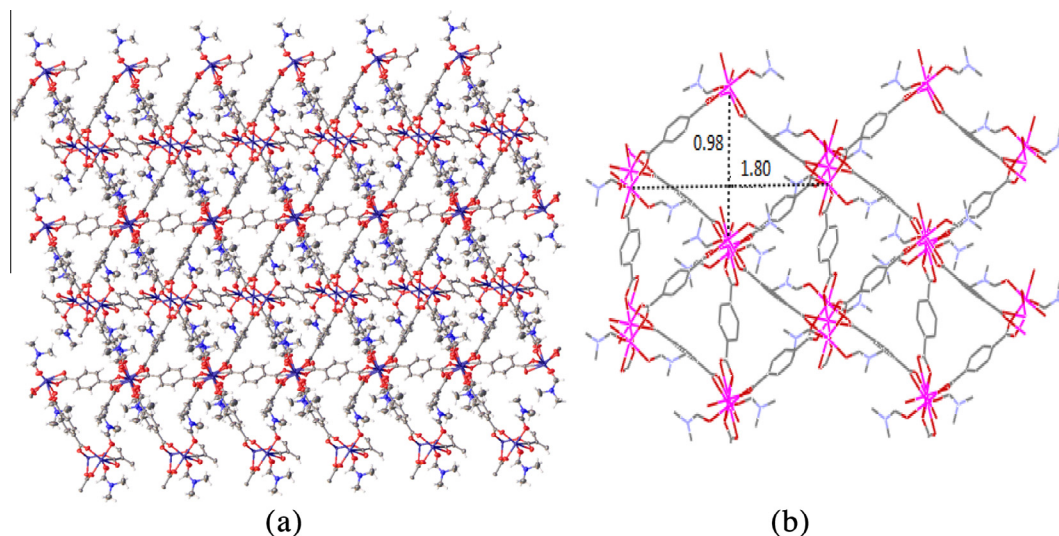


Fig. 4. View of (a) the 2D framework of $[\text{Mn}_3(\text{BDC})_3(\text{DMF})_4]_n$ (b) with the resulting channels having dimensions of 0.98×1.80 nm.

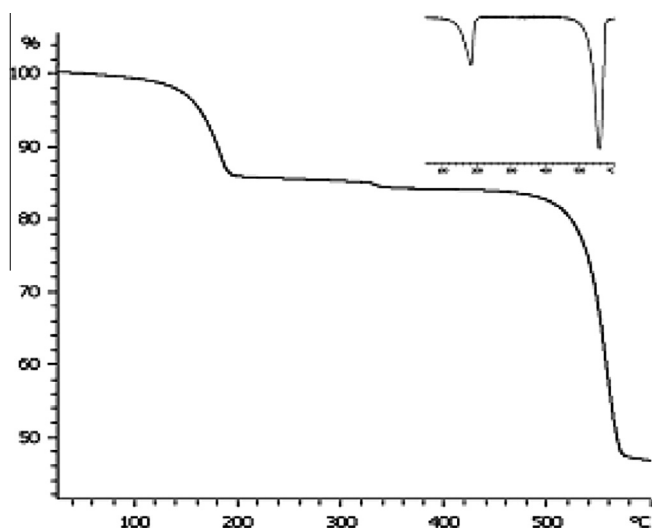


Fig. 5. TGA and DSC curves of the $[\text{Mn}_3(\text{BDC})_3(\text{DMF})_4]$ coordination polymer.

the Mn-terephthalate coordination polymer, different oxidants containing terminal hydroperoxides were considered. Various oxidants, including *tert*-butyl hydroperoxide (TBHP, 70% in water), urea hydrogen peroxide (UHP), cumene hydroperoxide (CHP) and hydrogen peroxide (H_2O_2 , 30%) for styrene oxidation over $[\text{Mn}_3(\text{BDC})_3(\text{DMF})_4]_n$ were tested and the results were 96%, 25%, 40% and 3% conversion, respectively. The difference in activity of UHP (as a source of hydrogen peroxide) and H_2O_2 (conversion 25 and 3% respectively) was due to the high amount of water in H_2O_2 and the hydrophobic nature of $[\text{Mn}_3(\text{BDC})_3(\text{DMF})_4]_n$. Moreover, UHP is not completely soluble in the 1,2-dichloroethane solvent. It seems that the steric effects of the phenyl group of cumene in CHP play a significant role in decreasing the reaction rate (conversion 40%). Clearly, TBHP was the most active oxidant, achieving 96% conversion within 9 h.

The temperature effect on the reaction was studied in the range 25–75 °C. The results indicated that when the temperature is increased up to 75 °C, the conversion (96%) of styrene clearly increased, whilst at room temperature a low conversion (2%) was detected.

After optimizing the reaction conditions, the process was extended to the oxidation of other substrates to their correspond-

Table 3

Effect of solvent on the oxidation of styrene, catalyzed by $[\text{Mn}_3(\text{BDC})_3(\text{DMF})_4]_n/\text{TBHP}^a$.

Selectivity to styrene oxide ^c (%)	Conversion ^b (%)	Solvent
42 (57) ^d	88	acetonitrile
58 (42) ^d	96	1,2-dichloroethane
–	2	methanol
56 (41) ^d	35	DMF
–	2	acetonitrile/methanol

^a Reaction conditions: catalyst 3 mg, styrene 1 mmol, TBHP 1 mmol, solvent 2 mL, temperature 75 °C, time 9 h, the molar ratio for catalyst:styrene:TBHP is 1:100:100.

^b Conversion determined by GC using chlorobenzene as an internal standard.

^c Selectivity (%) = (moles of styrene oxide/total moles of products) \times 100.

^d Selectivity to benzaldehyde as the other main product.

Table 4

Oxidation of olefins by $[\text{Mn}_3(\text{BDC})_3(\text{DMF})_4]_n/\text{TBHP}^a$.

Substrate	Conversion ^b (%)	Selectivity to epoxide (%)
Cyclooctene	66	86
Cyclohexene	66	1<
Styrene	96 (2) ^c	58(58) ^d
α -methylstyrene	89	75
<i>cis</i> -stilbene	30	100 (87) ^e
<i>trans</i> -stilbene	54	100 (100) ^e
Indene	77	100

^a Reaction conditions: the molar ratio for catalyst:substrate:*t*-BuOOH is 1:100:100. The reactions were run in 2 mL 1,2-dichloroethane at 75 °C for 9 h.

^b Conversion determined by GC using chlorobenzene as an internal standard.

^c The blank test without catalyst.

^d The reaction was done under an N_2 atmosphere.

^e Selectivity (%) to the *trans*-product.

ing products, as summarized in Table 4. The catalytic oxidation of various olefins, with TBHP as an oxidant, is effectively carried out with $[\text{Mn}_3(\text{BDC})_3(\text{DMF})_4]_n$. Oxidation of styrene by TBHP in the presence of $[\text{Mn}_3(\text{BDC})_3(\text{DMF})_4]_n$ in 1,2-dichloroethane involves C=C bond breaking, yielding benzaldehyde (42%) with styrene oxide (58%) within 9 h at 75 °C. Epoxidation of *trans*-stilbene led only to the *trans*-epoxide, while epoxidation of *cis*-stilbene produces *trans*-stilbene oxide (87%) and minor amounts of *cis*-stilbene oxide (12%) under similar conditions.

We aimed at pursuing the catalytic mechanism of this CP as a heterogeneous catalyst, so we examined the cyclohexene oxidation

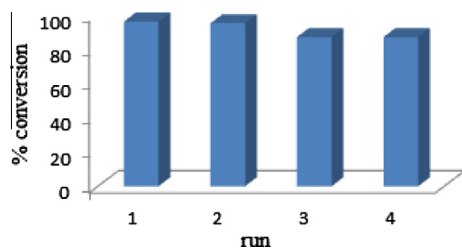


Fig. 6. Reusability studies of the $[\text{Mn}_3(\text{BDC})_3(\text{DMF})_4]_n$ catalyst for the oxidation of styrene by TBHP.

in the presence of this catalyst since it is a substrate that is particularly prone to allylic oxidation. Cyclohexene oxidation in the presence of $[\text{Mn}_3(\text{BDC})_3(\text{DMF})_4]_n$ provided 2-cyclohexene-1-ol (98%) and cyclohexene-1-one (2%) in 66% conversion. These products were observed for cyclohexene oxidation by other CPs as catalysts, such as $[\text{Cu}(\text{H}_2\text{btec})(\text{bpy})]$ (where H_4btec = 1,2,4,5-benzenetetracarboxylic acid and bpy = 2,2-bipyridine) [40] and $[\text{Ni}_2(\text{dhtp})(\text{H}_2\text{O})_2] \cdot 8\text{H}_2\text{O}$ (where dhtp = 2,5-dihydroxyterephthalate) [41]. These oxidation products strongly suggest a dominant radical pathway for this oxidation reaction, as was expected on the basis of earlier reports [42]. In agreement with the results observed in the cyclohexene oxidation, loss of stereoselectivity in the stilbene oxidation, a radical intermediate has been proposed which leads to *cis/trans*-epoxides through isomerization by simple bond rotation [43–45].

To explore the in situ formation of radical species in the oxidation reaction, ionol (2,6-di-*tert*-butyl-*p*-cresol) was used as a radical scavenger in the oxidation of styrene and cyclohexene. Oxidation was completely inhibited in the presence of ionol (conversion 7% for styrene oxidation and 5% for cyclohexene oxidation). The effective inhibition of oxidation by ionol confirmed the formation of a radical intermediate in the reaction pathway. This evidence indicates that in the present manganese/*t*-BuOOH oxidation system the radical process is initiated by the homolytic cleavage of the O–O bond of *t*-BuOOH, which is catalyzed in the presence of the manganese complex. As a previously reported study emphasized [46], the low bond dissociation energy and activation energy for O–O bond cleavage in *t*-BuOOH probably makes the Mn–O–O–*t*-Bu moiety more easily undergo homolytic O–O bond cleavage. The result for styrene oxidation in the presence of the manganese/ H_2O_2 system (conversion 3%) is evidence for the easy break-

age of the O–O bond of Mn–O–O–*t*-Bu rather than Mn–O–O–H, which desires a radical pathway for the *t*-BuOOH oxidant.

3.4. Recyclability of the $[\text{Mn}_3(\text{BDC})_3(\text{DMF})_4]_n$ catalyst

The recyclability of a catalyst is a prominent feature of heterogeneous catalysis reactions. To investigate the reusability of the $[\text{Mn}_3(\text{BDC})_3(\text{DMF})_4]_n$ catalyst, the CP was easily isolated from the reaction mixture by simple filtration after the first catalytic reaction in the oxidation of styrene. It was recovered by being washed with solvent and dried at room temperature, then used for the next run under the same reaction conditions. The catalytic activity was found to remain almost the same, without any significant degradation in activity even after the fourth reaction (Fig. 6), but the selectivity changed to benzaldehyde as the sole product. As Jianglei et al. previously reported, the formation of benzaldehyde as the dominant product in later runs can indicate the catalytic reaction pathway is sterically controlled [47].

The hot filtration test was conducted to confirm that the reaction was indeed catalyzed by $[\text{Mn}_3(\text{BDC})_3(\text{DMF})_4]_n$ instead of free manganese. After the first catalytic reaction, the catalyst was simply separated from the reaction mixture by centrifugation. The fresh reagents were then added to the filtrated solution. The resulting mixture was stirred at 75 °C. The conversion was negligible after 12 h. These results confirmed the oxidation reaction could only proceed in the presence of the solid catalyst, and there was no contribution from leached manganese species in the liquid phase. Also, a leaching test after each catalytic run in the styrene oxidation reaction by $[\text{Mn}_3(\text{BDC})_3(\text{DMF})_4]_n/\text{TBHP}$ revealed that the amount of manganese leached from the catalyst to the solution is less than 1 ppm.

The crystalline structure of the CP was examined by XRD diffraction to validate the stability of the Mn CP after a catalytic run. In Fig. 7, the XRD pattern of Mn CP is shown before and after catalysis. The XRD pattern of the CP partially changes after the first catalytic run (Fig. 7b) compared to the fresh catalyst (Fig. 7a). The appearance of some new diffraction peaks after the first catalytic run can be attributed to the released 1,4-benzendicarboxylic acid linkers. This observation indicates that the structure is partially decomposed because of the TBHP/water mixture [48]. This also explains the relative Mn-leaching that was observed (the detection of less than 1 ppm of manganese by the hot filtration test).

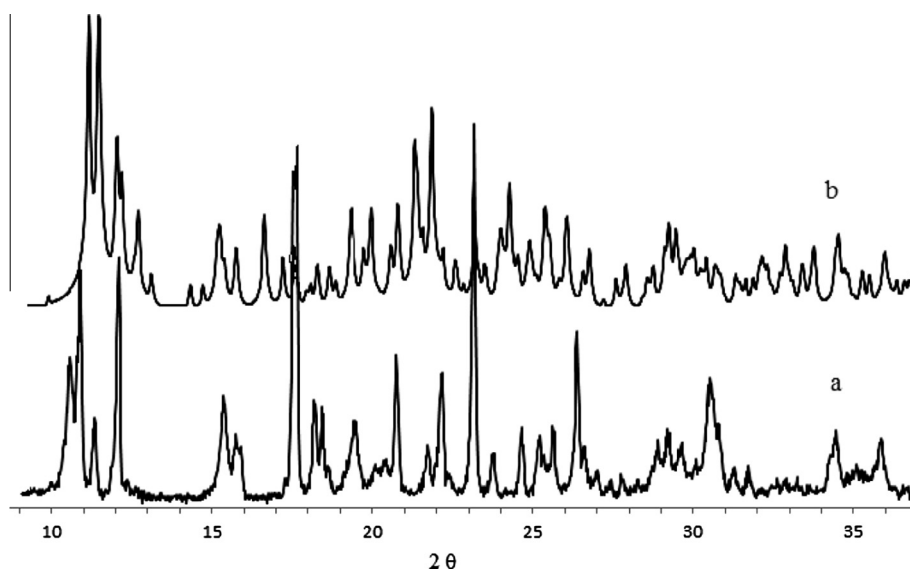


Fig. 7. XRD patterns of the fresh (a) and reused (b) catalyst.

4. Conclusion

The CP of $[\text{Mn}_3(\text{BDC})_3(\text{DMF})_4]_n$ was synthesized by a hydrothermal method. Single crystal structure analysis of the compound revealed that the complex crystallizes in the triclinic $P\bar{1}$ space group with a 2D infinite network composed of M–O–C units. A TGA study emphasized the stability of this metal complex. The catalytic oxidation of various olefins with TBHP was effectively carried out with $[\text{Mn}_3(\text{BDC})_3(\text{DMF})_4]_n$. The results of the catalytic study exhibited that the heterogeneous complex of $[\text{Mn}_3(\text{BDC})_3(\text{DMF})_4]_n$ is an active and selective catalyst for olefin oxidation with the TBHP oxidizing agent in 1,2-dichloroethane solvent. The reaction of cyclohexene with TBHP gives 2-cyclohexene-1-ol and cyclohexene-1-one. Also, styrene oxidation gives benzaldehyde and styrene oxide. The reaction products suggest the catalytic reactions probably proceed through a radical mechanism. Furthermore, addition of ionol (2,6-di-tertbutyl-p-cresol) as a radical scavenging species quenched the formation of the oxidation products, confirming the proposed radical mechanism. The CP catalyst was also found to be reusable for the oxidation of styrene several times, with a conversion ranging from 96% to 87% on the fourth run. The XRD analysis indicates that the framework of the complex does not undergo any significant structural change during catalysis.

Acknowledgements

M.B. acknowledges the research council of Sharif University of Technology for the research funding of this project. M.D. acknowledges the financial support of this research by the Ministry of Science, Education and Sport of the Republic of Croatia, Zagreb (Grant No. 119-1193079-1332).

Appendix A. Supplementary data

CCDC 882937 contains the supplementary crystallographic data for this paper, which can be obtained free of charge via www.ccdc.cam.ac.uk/data_request/cif [Cambridge Crystallographic Data Centre (CCDC), 12 Union Road, Cambridge CB2 1EZ, UK; Fax: +44 1223 336033; email: data_request@ccdc.cam.ac.uk].

References

- [1] S. Kitagawa, R. Kitaura, S.I. Noro, *Angew. Chem., Int. Ed.* 43 (2004) 2334.
- [2] R.J. Kuppler, D.J. Timmons, Q.R. Fang, J.R. Li, T.A. Makal, M.D. Young, D. Yuan, D. Zhao, W. Zhuang, H.C. Zhou, *Coord. Chem. Rev.* 253 (2009) 3042.
- [3] G. Mahmoudi, A. Morsali, A.D. Hunter, M. Zeller, *CrystEngComm* 9 (2007) 704.
- [4] A. Morsali, M.Y. Masoumi, *Coord. Chem. Rev.* 253 (2009) 1882.
- [5] C. Janiak, *Dalton Trans.* (2003) 2781.
- [6] Y. Shibata, *J. Coll. Sci.* 37 (1916) 1.
- [7] W.W. Dong, J. Zhao, L. Xu, *J. Solid State Chem.* 181 (2008) 1149.
- [8] Z. Chen, X. Li, F. Liang, *J. Solid State Chem.* 181 (2008) 2078.
- [9] H.L. Gao, L. Yi, B. Zhao, X.Q. Zhao, P. Cheng, D.Z. Liao, S.P. Yan, *Inorg. Chem.* 45 (2006) 5980.
- [10] B.L. Chen, F.R. Fronczek, A.W. Maverick, *Inorg. Chem.* 43 (2004) 8209.
- [11] C.D. Wu, W.B. Lin, *Chem. Commun.* (2005) 3673.
- [12] M. Afsharpour, A.R. Mahjoub, M.M. Amini, *Appl. Catal. A: Gen.* 327 (2007) 205.
- [13] K. Seki, W. Mori, *J. Phys. Chem. B* 106 (2002) 1380.
- [14] L. Zhang, Y. Ling, A. Hu, T. Yao, J. Li, *Inorg. Chim. Acta* 362 (2009) 4867.
- [15] Y. Sun, S. Wang, K. Li, E. Gao, G. Xiong, M. Guo, Z. Xu, Y. Tian, *Inorg. Chem. Commun.* 28 (2013) 1.
- [16] J.X. Li, Z.X. Du, J.G. Wang, T. Wang, J.N. Lv, *Inorg. Chem. Commun.* 15 (2012) 243.
- [17] H. Xu, Y. Song, H. Hou, *Inorg. Chim. Acta* 357 (2004) 3541.
- [18] J. Jin, D. Li, L. Li, X. Han, S. Cong, Y. Chi, S. Niu, *Inorg. Chim. Acta* 379 (2011) 44.
- [19] X. Zhang, Y. Huang, Y. Yao, *Inorg. Chem. Commun.* 28 (2013) 49.
- [20] C.S. Hawes, C.M. Fitchett, S.R. Batten, P.E. Kruger, *Inorg. Chim. Acta* 389 (2012) 112.
- [21] S. Konar, A. Jana, K. Das, S. Ray, S. Chatterjee, S.K. Kar, *Inorg. Chim. Acta* 395 (2013) 1.
- [22] J. Liu, Y. Wang, Y. Huang, *CrystEngComm* 13 (2011) 3733.
- [23] G. Mahmoudi, A. Morsali, *CrystEngComm* 9 (2007) 1062.
- [24] D.M.J. Dobe, C.H. Benison, A.J. Blake, D. Fenske, M.S. Jackson, R.D. Kay, W. Li, M. Schroder, *Angew. Chem., Int. Ed.* 38 (1999) 1915.
- [25] Y. Tokunaga, D.M. Rudkevich, J. Rebek Jr., *Angew. Chem., Int. Ed.* 36 (1997) 2656.
- [26] M.A. Withersby, A.J. Blake, N.R. Champness, P. Hubberstey, W.S. Li, M. Schroder, *Angew. Chem., Int. Ed.* 36 (1997) 2327.
- [27] O.M. Yaghi, H. Li, *J. Am. Chem. Soc.* 117 (1995) 10401.
- [28] Z. Hnatejko, G. Dutkiewicz, M. Kubicki, S. Lis, *J. Mol. Struct.* 1034 (2013) 128.
- [29] J. Yang, H. Chen, T.H. Lo, *Inorg. Chem. Commun.* 14 (2011) 217.
- [30] A. Das, G. Pilet, D. Luneau, M.S. Fallah, J. Ribas, S. Mitra, *Inorg. Chim. Acta* 358 (2005) 4581.
- [31] J.M. Rueff, N. Masciocchi, P. Rabu, A. Sironi, A. Skoulios, *Eur. J. Inorg. Chem.* (2001) 2843.
- [32] L.T.L. Nguyen, T.T. Nguyen, K.D. Nguyen, N.T.S. Phan, *Appl. Catal. A: General* 425 (2012) 44.
- [33] N.T.S. Phan, K.K.A. Le, T.D. Phan, *Appl. Catal. A: Gen* 382 (2010) 246.
- [34] Oxford Diffraction, Version 171.31 Oxford Diffraction Ltd., Xcalibur CCD System, CrysAlis, 2004.
- [35] O.V. Dolomanov, L.J. Bourhis, R.J. Gildea, J.A.K. Howard, H. Pushmann, *J. Appl. Crystallogr.* 42 (2009) 339.
- [36] G.M. Sheldrick, *Acta Crystallogr., Sect. A* 64 (2008) 112.
- [37] N.L. Rosi, J. Kim, M. Eddaoudi, B. Chen, M. O'Keeffe, O.M. Yaghi, *J. Am. Chem. Soc.* 127 (2005) 1504.
- [38] F. Luo, Y. Che, J. Zheng, *Inorg. Chem. Commun.* 11 (2008) 358.
- [39] S.Y. Yang, H.B. Yuan, X.B. Xu, R.B. Huang, *Inorg. Chim. Acta* 403 (2013) 53.
- [40] K. Brown, S. Zolezzi, P. Aguirre, D. Venegas-Yazigi, V. Paredes-García, R. Baggio, M.A. Novak, E. Spodine, *Dalton Trans.* (2009) 1422.
- [41] J.S. Lee, S.B. Halligudi, N.H. Jang, D.W. Hwang, J.S. Chang, Y.K. Hwang, *Bull. Korean Chem. Soc.* 31 (2010) 1489.
- [42] M. Bagherzadeh, M. Zare, *J. Coord. Chem.* 65 (2012) 4054.
- [43] W. Adam, K.J. Roschmann, C.R. Saha-Möller, D. Seebach, *J. Am. Chem. Soc.* 124 (2002) 5068.
- [44] W. Adam, K.J. Roschmann, C.R. Saha-Möller, *Eur. J. Org. Chem.* (2000) 3519.
- [45] M. Palucki, N.S. Finney, P.J. Pospisil, M.L. Guler, T. Ishida, E.N. Jacobsen, *J. Am. Chem. Soc.* 120 (1998) 949.
- [46] G. Yin, A.M. Danby, D. Kitko, J.D. Carter, W.M. Scheper, D.H. Busch, *Inorg. Chem.* 46 (2007) 2173.
- [47] H. Jianglei, L. Kexin, L. Wei, M. Fengyan, G. Yihang, *Appl. Catal. A: Gen.* 364 (2009) 211.
- [48] K. Leus, M. Vandichel, Y. Liu, I. Muylaert, J. Musschoot, S. Pyl, H. Vrielinck, F. Callens, G.B. Marin, C. Detavernier, P.V. Wiper, Y.Z. Khimyak, M. Waroquier, V.V. Speybroeck, P. Van Der Voort, *J. Catal.* 285 (2012) 196.